Radiotherapy and Oncology 137 (2019) 130–136

Contents lists available at ScienceDirect

Radiotherapy and Oncology

journal homepage: www.thegreenjournal.com

Original Article

The first prototype of spot-scanning proton arc treatment delivery

Xiaoqiang Li [a,*], Gang Liu [a,b,c], Guillaume Janssens [d], Olivier De Wilde [d], Vincent Bossier [d], Xavier Lerot [d], Antoine Pouppez [d], Di Yan [a], Craig Stevens [a], Peyman Kabolizadeh [a], Xuanfeng Ding [a,*]

[a] Department of Radiation Oncology, Beaumont Health System, Royal Oak, USA; [b] Cancer Center, Union Hospital, Tongji Medical College, Huazhong University of Science and Technology; [c] School of Physics and Technology, Wuhan University, Wuhan, China; and [d] Advanced Technology Group, Ion Beam Applications SA, Louvain-la-Neuve, Belgium

ARTICLE INFO

Article history:
Received 24 December 2018
Received in revised form 27 March 2019
Accepted 25 April 2019
Available online 14 May 2019

Keywords:
Spot scanning
Proton arc therapy
Quality assurance

ABSTRACT

Purpose: We report the first prototype of spot-scanning arc treatment (SPArc) delivery on a clinical proton beam therapy machine and evaluate its delivery accuracy and efficiency.

Methods and materials: A new module called Proton Dynamic Arc Delivery (PDAD) was developed to allow simultaneously delivering spot-scanning proton beam treatments while rotating the gantry on an IBA Proteus®One proton machine. A series of measurements was performed to validate the basic beam characteristics. Subsequently, patient specific quality assurance (QA) of a brain SPArc plan was performed. Total SPArc treatment delivery time was also recorded and compared to the clinically delivered intensity modulated proton therapy (IMPT) treatment time. Finally, the log file of the SPArc plan was analyzed and processed to reconstruct the actual delivered dose.

Results: All the basic beam characteristics were confirmed in the PDAD mode, similar as those measured using fixed gantry deliveries in clinical mode. The brain SPArc plan with similar or superior plan quality was delivered in 4 mins compared to total 11 mins for the clinical treatment of the three-field IMPT plan. The patient QA result showed a good agreement between the measured and calculated dose distributions with the gamma index of 98.6% (3%/3 mm). The analysis of the log file confirmed the accuracy of the SPArc plan delivery, with the gamma index of 98.3% (1%/1 mm) between reconstructed and the planned doses.

Conclusion: The first prototype of dynamic proton arc delivery on a clinical proton therapy system was successfully performed. The measurements and simulations demonstrated the feasibility of SPArc treatment within the clinical requirements.

© 2019 Elsevier B.V. All rights reserved. Radiotherapy and Oncology 137 (2019) 130–136

Pencil beam scanning (PBS) technique [1,2] has become a popular treatment modality in proton therapy [3], which offers superior dosimetric properties compared to photon therapy and passive scatter proton beam therapy [4–7]. In PBS, the narrow beams (spots) deliver the therapeutic radiation dose from several fixed beam directions via spots in an optimized fashion. However, the dosimetric quality of the PBS plan could be limited [8] due to the large lateral penumbra [9], uncertainties from patient's daily setup and proton range [10–16], and limited angles for delivery given the treatment delivery efficiency [17–19]. Recently, spot-scanning proton arc therapy (SPArc) technique has been proposed to further improve plan quality, robustness, and delivery efficiency [20].

SPArc is a novel and an advanced form of intensity modulated proton therapy (IMPT) planning and treatment approach, in which the planning optimization algorithm selects the energies and positions of spots along a dynamic rotational arc trajectory. Such robust optimized and delivery-efficient SPArc plan based on hundreds of control points could potentially enable the proton system to deliver proton arc therapy in a continuous rotation gantry mode while avoiding the dose to organs-at-risk (OARs). SPArc planning algorithm starts from robust optimization with a coarse angle sampling and then increases the sampling rate iteratively while filtering energy layers, spots and re-distributing the energy layers, spots to further optimize the plan quality, robustness, and arc treatment delivery efficiency simultaneously [20]. As it was reported previously, SPArc has a greater ability to improve the plan quality and robustness in multiple disease sites such as prostate, lung, and head and neck cancers compared to multi-field robust optimized IMPT [8,21,22]. Although previous SPArc studies have been centered on dosimetric simulations, there are still many technical challenges to implement such continuous gantry rotation with scanning proton beam delivery [21]. These challenges include the degree of accuracy to control and monitor the speed and the position of the proton gantry in real-time; the capability of delivering

* Corresponding authors at: Department of Radiation Oncology, Beaumont Health System, Royal Oak, MI, USA.
E-mail addresses: Xiaoqiang.Li@beaumont.org (X. Li), Xuanfeng.Ding@beaumont.org (X. Ding).

https://doi.org/10.1016/j.radonc.2019.04.032
0167-8140/© 2019 Elsevier B.V. All rights reserved.

spots within sub-millimeter accuracy during dynamic gantry rotation mode and switching the energy layers efficiently between each gantry rotation control point. Recently, IBA (Ion Beam Applications, Louvain-La-Neuve, Belgium) has developed a new scanning beam control module within the existing hardware in our clinical proton beam therapy system. Such research treatment module allows the beamline to deliver scanning proton beam while continuously rotating the gantry. The purpose of this study is to design and implement procedures to quantitatively evaluate the performance of this novel SPArc treatment delivery using a clinical proton beam therapy system.

Methods and materials

IBA Proteus®One proton therapy system

Our proton beam therapy system consists of an IBA superconducting synchrocyclotron (S2C2) [23] and a Proteus®One 220 degree compact gantry with a dedicated scanning beam nozzle to deliver proton beam energy from 70 to 227.7 MeV. The corresponding spot size in terms of one sigma in air at isocenter plane ranges from 0.8 cm to 0.3 cm, respectively. The maximum field size of the proton unit is 20×24 cm^2 at isocenter.

IBA Proton Dynamic Arc Delivery

IBA Proton Dynamic Arc Delivery (PDAD) system is a new beam delivery module which allows delivering spot scanning beams while continuously rotating the gantry. Currently, the PDAD module is a prototype system operating in research mode. SPArc plan consists of a sequence of proton arc delivery control points, for which the gantry angle, spot positions and energies, and monitor units (MUs) are defined. The PDAD system calculates the delivery sequences based on the pre-defined parameters which include the minimum and maximum gantry speeds of 0.1 degree/s and 2 degree/s, the estimated energy layer switching time from high to low energy (0.6 s) and from low to high energy (5.5 s), the estimated scanning delivery time of each control point, and an adjustable angular tolerance between the actual delivered and planned gantry angles. The angular tolerance defines an angular window during which an arc delivery control point can be delivered. This tolerance was set to 1 degree in this study (angular window of ±1 degree around the planned angle). The delivery is synchronized to the gantry position by the PDAD controller, so that the control point is delivered within the angular window. The estimated delivery time of the control points and the layer switching time determine the gantry rotation speed at a given angle.

Proton arc beam characteristic tests

Under the prerequisites of the standard machine QAs [24], a series of tests for different energies of 70, 120, 180, and 227.7 MeV proton beam has been performed to validate the beam characteristics, accuracy and stability under the PDAD module. These consisted of radiation isocentricity, spot profile, beam flatness and symmetry, and beam output.

Isocentricity

The isocentricity of the arc delivery was evaluated by delivering only central spots (2MU per spot with 5 degree gantry spacing) while gantry continuously rotating clockwise from 330 degree to 180 degree. The positions of the central spots in three directions and gantry angles were measured at isocenter using XRV100 scintillator (Logo System Intl, CA, USA) (Fig. 1a) [25]. The change in spot positions over gantry angles was recorded.

Spot profiles

The single spot profiles at different gantry angles through the arc delivery were measured in air at isocenter plane using a gantry mounted scintillator-based Lynx detector (IBA Dosimetry, Schwarzenbruck, Germany) (Fig. 2a) [26,27]. The baseline measurements were also acquired with the same setup using static mode at several selected gantry angles (330, 0, 45, 90, 135, and 180 degrees) in clinical mode which were compared to the spot profiles in the PDAD mode.

Proton beam flatness and symmetry

10×10 cm^2 square fields consisting of 1681 spots with 2.5 mm spot spacing (1MU per spot, total 1681 MUs) were processed (see Fig. 2 of Supplementary materials) to create the arc fields by distributing the spots equally to all the control points (5 degree spac-

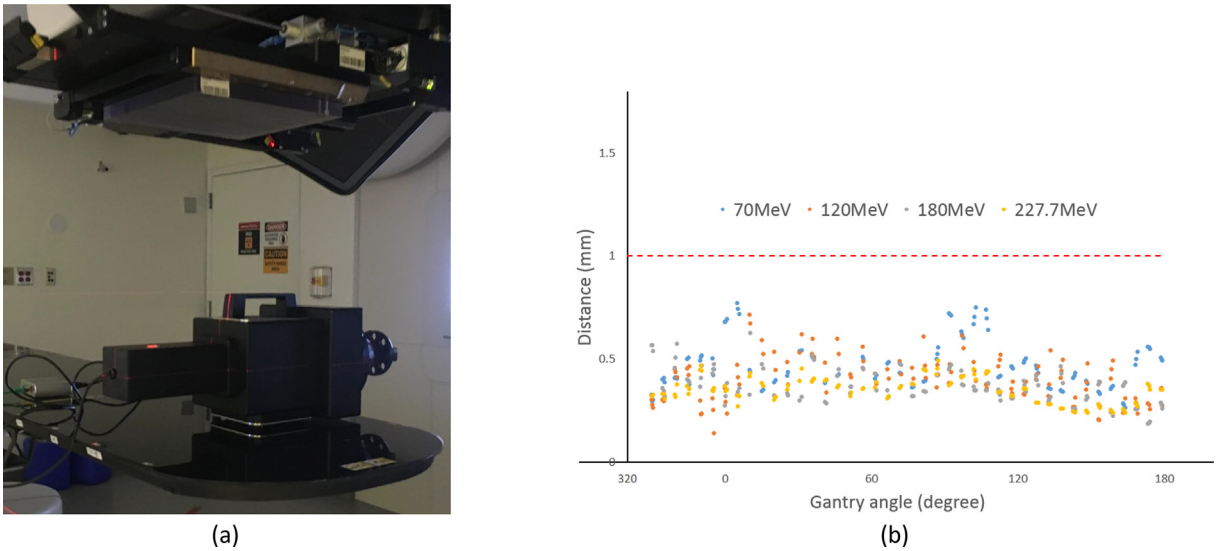

Fig. 1. (a) The setup to measure the isocentricity using XRV100. (b) The change in the center of the central spot relative to iso-center acquired from a clockwise arc delivery from 330 to 180 degree.

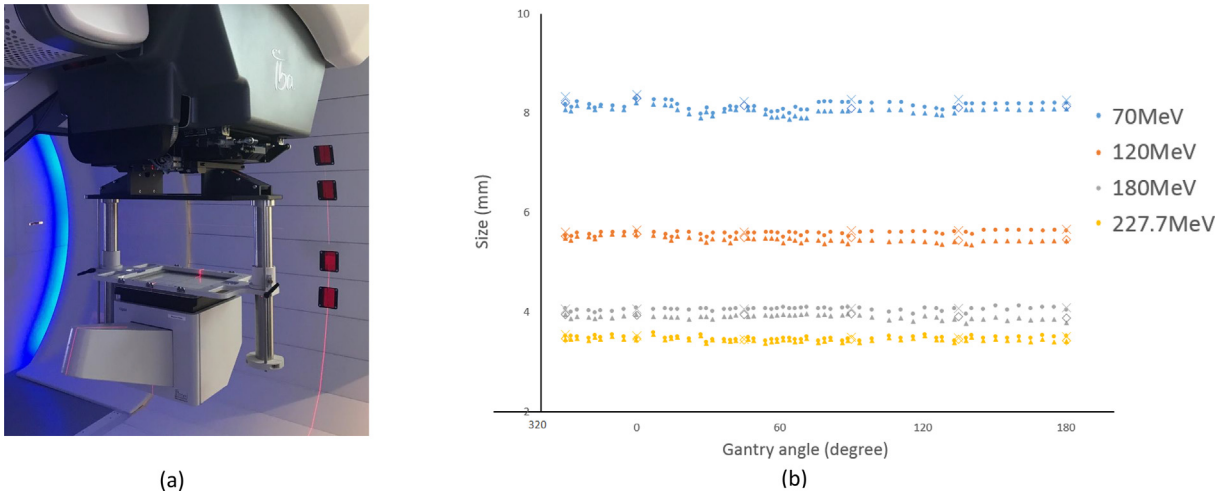

Fig. 2. (a) The setup to measure spot sizes using Lynx mounted on the gantry. (b) The spot profiles in X (triangle and square) and Y (dot and cross) directions in terms of one sigma in air at isocenter plane acquired in arc (triangle and dot) and static (square and cross) mode.

ing) following the delivery pattern. These fields were delivered in the PDAD mode and measured via a two-dimensional ionization chamber detector array, MatriXXOne (IBA Dosimetry, Schwarzenbruck, Germany) with 2 cm solid water buildup. The MatriXXOne was mounted to the gantry using a special designed holder (Fig. 3a), which was located at beam isocenter plane and rotated with the gantry. The beam flatness and symmetry of those fields were analyzed and compared with the baseline profiles acquired under the static mode delivered at gantry zero degree.

Proton Arc delivery output

The same $10 \times 10\ cm^2$ fields were used to measure the beam output during the arc delivery. The dose was measured using a calibrated PPC-05 parallel chamber (IBA Dosimetry, Schwarzenbruck, Germany) at the depth of 2.7 cm of solid water material, which was mounted to the gantry at the isocenter plane read by a Dose 1 Electrometer (IBA Dosimetry, Schwarzenbruck, Germany). The output acquired by delivering the same fields at gantry zero degree was analyzed to evaluate the output consistence under the PDAD mode.

Patient SPArc plan delivery

One brain patient who underwent a three-beam (including one vertex beam) IMPT treatment at our center was re-planned with a partial arc (2.5 degree spacing) with gantry clockwise rotation from 40 to 180 via energy layer delivery optimized SPArc algorithm [28]. The SPArc plan was optimized using worst-case robust optimization with the same uncertainties parameters (±3mm setup and ±3.5% range uncertainties, total 21 scenarios) to achieve similar clinical target volume (CTV) robust coverage as the clinical plan. The total number of control points, energy layers, and spots was 50, 97, and 4783 respectively. The brain SPArc plan was then transferred to IBA Proteus®One treatment system and delivered in the PDAD mode. Total delivery time was recorded and compared with the average clinical treatment delivery time for this patient.

Patient specific QA

The patient specific plan QA was performed using MatriXXOne mounted to the gantry (Fig. 3a) with 2 cm solid water buildup. The gamma index [29] using 3% and 3 mm criteria was used to evaluate the measured and calculated 2D dose distributions.

Log analysis and dose reconstruction

During the SPArc plan QA delivery in Section (Patient specific QA), the treatment log file recorded the actual delivered position, MUs, time, and the corresponding gantry angle of each spot. This log file was extracted to analyze the actual energy switching time,

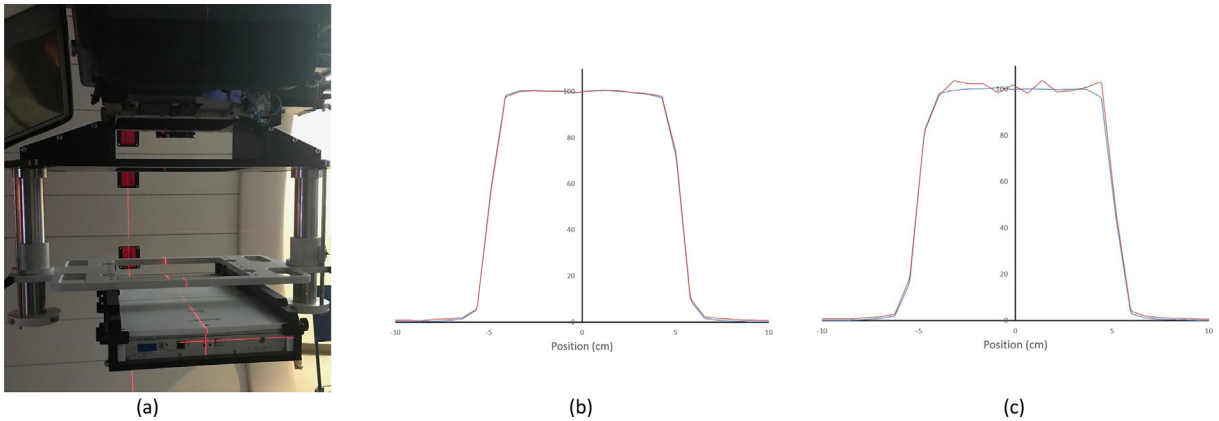

Fig. 3. (a) The gantry mounted setup to measure the flatness and symmetry using MatriXXOne. The profiles in (b) X and (c) Y directions for a $10 \times 10\ cm^2$ field measured using MatriXXOne with 2 cm solid water buildup for arc (red) and static (blue) delivery. (For interpretation of the references to colour in this figure legend, the reader is referred to the web version of this article.)

the gantry speed, and the MUs delivered at each angle. The delivered dose was also reconstructed by computing the dose on the initial planning CT in treatment planning system (TPS) based on the actual delivered information from log file [30–32]. The dose distributions and dose–volume histograms (DVHs) were compared for the reconstructed and planned doses. The 3D gamma index using 1% dose and 1 mm criteria was also assessed.

Results

Proton Arc beam characteristics

Isocentricity

Fig. 1b shows the central spot positions relative to the iso-center delivered in arc mode from 330 to 180 degree for energies of 70, 120, 180, and 227.7 MeV. All the spots were delivered at the gantry angles within ±1 degree of the planned gantry angle. All the spots were within 1 mm position accuracy, while the maximum deviation from the iso-center was 0.77 mm for the 70 MeV.

Spot profiles

Fig. 2b shows the spot sizes in both X and Y directions delivered in arc and static modes. The average spot sizes for X and Y directions were 0.80 and 0.82 cm, 0.55 and 0.56 cm, 0.39 and 0.41 cm, 0.34 and 0.35 cm for energies of 70, 120, 180, and 227.7 MeV using arc delivery mode. The maximum standard deviation for the spot size from different gantry angles was 1.1%. Compared to the results acquired in static mode, the spot sizes were consistent within 1.5%.

Beam flatness and symmetry

Generally, the symmetry of the square fields measured in the dynamic arc mode was very similar to the static mode, with the differences in X and Y directions being 0.04% and 0.01%, 0.05% and 0.09%, 0.08% and 0.4%, 0.01% and 0.1% respectively for energies of 70, 120, 180, and 227.7 MeV. The differences of the flatness in X and Y directions between arc and static delivery mode evaluated with 2 cm solid water buildup were within 0.6% except for the flatness in Y direction for 227.7 MeV energy of 2.2% (Fig. 3c).

Proton arc output

The output measured for the square fields were compared between the arc and static delivery modes. The result showed the difference of 1.84%, −0.40%, 0.96%, and −0.53% for energies of 70, 120, 180 and 227.7 MeV, respectively. These findings suggest that the beam output is stable and reliable during the arc delivery.

Patient SPArc plan

The dose distributions and DVHs of the three-field (two co-planar and one vertex) IMPT and the SPArc plans for the brain case are shown in Fig. 4. The SPArc plan was able to achieve similar or superior plan quality and robustness (Fig. 1 of Supplementary materials) without using a non-coplanar beam. Compared with the IMPT plan with a couch kick, which took an average of 11 min to deliver, the SPArc could finish the delivery in 4 min. This is just to demonstrate the significant benefit of arc therapy in terms of treatment delivery efficiency and workflow in complicated clinical cases compared to the current clinical practice.

Patient specific quality assurance

Fig. 5a shows the planar iso-dose lines comparison for the calculated and measured SPArc with 2 cm solid water buildup. Fig. 5b shows the gamma index map calculated with 3% and 3 mm between the two doses. The gamma index reached 98.6%, which indicates the good agreement between the calculated and measured doses.

Log analysis and dose reconstruction

According to the log file, all the spots were delivered within the tolerance of the planned gantry angles ±1 degree (Fig. 3 of Supplementary materials). The observed energy layer switching time was between 0.35 and 0.55 s for energy switching downward, and between 3.5 and 5.5 s for energy switching upward. The minimum and maximum gantry speed during the SPArc irradiation were 0.14 and 1.58 degree/s (Fig. 6a). Fig. 6b shows the DVHs comparisons for target and several OARs between the planned and the log recon-

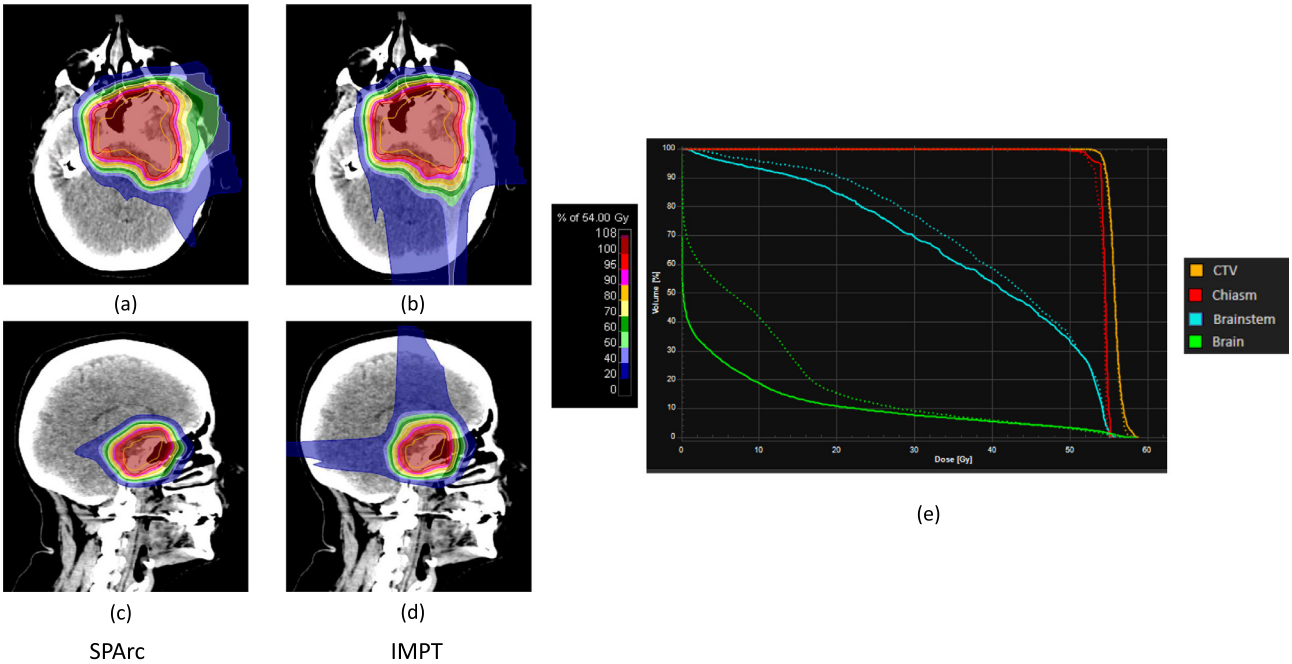

Fig. 4. The dose and DVHs (solid for SPArc, dashed for IMPT) comparisons between the SPArc ((a) and (c)) and IMPT ((b) and (d)) plans in a patient with brain tumor.

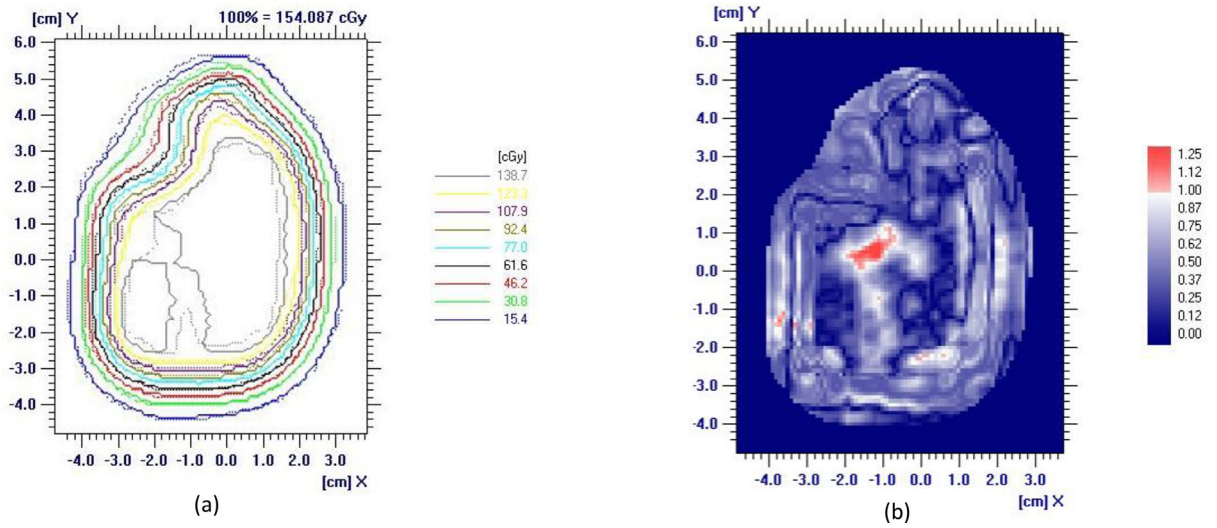

Fig. 5. (a) The iso-dose lines comparison for measured (solid) and calculated (dashed) doses. (b) The gamma index map using 3% and 3 mm criteria between measured and calculated doses.

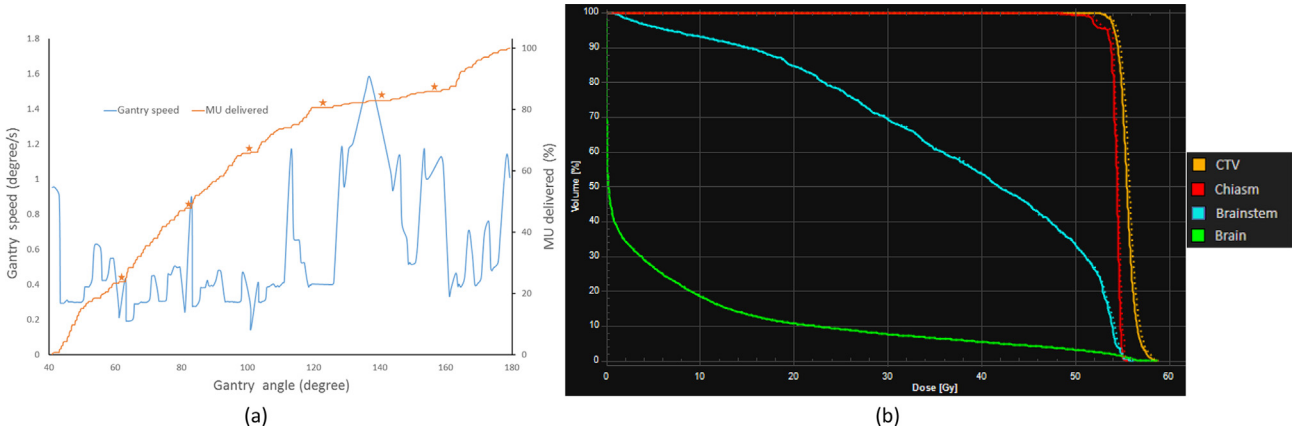

Fig. 6. (a) The gantry speed calculated from log-file (blue line) and the cumulative MUs (orange) delivered relative to the gantry angle, where stars stand for the angle where energy switches from low to high. (b) The DVHs comparisons from the log file for reconstructed (solid) vs planned (dashed) doses. (For interpretation of the references to colour in this figure legend, the reader is referred to the web version of this article.)

structed doses. The maximum difference between the two doses in target was 0.2%. The gamma index using 1% and 1 mm criteria was 98.3% between reconstructed and plan doses.

Discussion

Since the initial introduction of proton arc treatment technique, SPArc has demonstrated its capability to further improve the plan quality, robustness, and delivery efficiency in various treatment sites compared to current standard technique of robust optimized multi-field IMPT plans [8,21,22]. However, in order to deliver SPArc plans, the proton gantry requires to be capable of rotating around the iso-center while delivering small pencil beams within sub-millimeter accuracy. The study evaluates the first prototype arc delivery using a clinical proton therapy machine. Our preliminary results demonstrated that the spot-scanning arc delivery could be achieved with similar accuracy as the current PBS technique without modifying the hardware in existing clinical proton machine. Although this is a prototype tested in the research mode without implementing the required beam interlocks and safety checks, the experiment results demonstrated the feasibility and accuracy of such continuous proton arc delivery.

Moreover, a small difference was detected for beam flatness in Y direction (Fig. 3(c)) for only 227.7 MeV energy between the arc and static deliveries. This discrepancy is dependent on the sequence of beam delivery, where spots in different Y direction were given from different control points. Due to small uncertainties of the spot positions (Fig. 1b) from different gantry angles, the beam profile showed some wavelike changes (Fig. 3c). However, this discrepancy could not be clinically significant since the measurement was completed with 2 cm buildup which is away from the Bragg Peak region. Moreover, this difference can be washed out as the spot size becomes larger or depth closer to the Bragg Peak, which could be concluded by the smaller differences in beam flatness of other three lower energy measurements.

In this study, energy sorting SPArc algorithm was used to improve the SPArc delivery efficiency [28]. Compared to the original SPArc algorithm [20], which re-distributed the energy layers randomly without any orders to new sub-control points, the new algorithm starts from coarser sampling angles (20 degree), and re-distributes the energy layers with an order following the gantry

rotational direction. This minimized the number of energy switches from low to high energies resulting in achieving a similar plan quality while significantly decreasing the proton arc therapy delivery time.

In the current PDAD mode, the static control points are converted to delivery sequences and the pre-defined parameters (*e.g.*, gantry angle deviation window, gantry speed, energy switching time) are set to be conservative in order to ensure the proton arc delivery accuracy in this first prototype. For instance, the extent of the gantry deviation window is set to be 1 degree. This tolerance could be a variable number depending on the beam path inhomogeneity, the number of spots, energy layers, and MUs of each control points, and gantry sampling rate. Through further optimization of these parameters, the proton arc delivery efficiency could be improved while maintaining similar delivery accuracy.

The accuracy of arc delivery could be affected by the gravity force, especially in case of proton gantry. In Proteus®One system, the gantry angle dependent scanning magnet is used to correct the gantry sagging. During the arc delivery, the PDAD module interpolates the scanning table and effectively tunes the beam to maintain the isocentricity between each control point. In addition, the sagging of the measurements device mounted to the gantry could possibly affect the measurement results. In our analysis, although the patient QA for the SPArc passed our criteria (95%), depending on the plan complexity and sag magnitude, we may need to implement a gantry sagging correction algorithm or develop some new measurement device to compensate such effect.

One of the limitations of this study is that only basic spot characteristic analysis and single depth 2D measurements due to design of the MatriXXOne holder were completed to verify the accuracy of the arc delivery. Although the findings seem very promising, more beam measurements (*e.g.*, deeper depth measurement, range verification during arc delivery) and patient specific QAs are still required to perform a comprehensive analysis on consistency, accuracy and stability of the proton arc delivery. Lastly, new procedures and devices need to be designed to make this quality assurance more accurate and efficient.

In order to implement proton arc prototype for clinical use, there are still some issues to solve such as (1) Improving the stability of the machine and reducing the beam pauses as much as possible; (2) implementing procedures for beam pauses to resume the arc delivery; (3) designing the safety interlock for the arc delivery; (4) developing new DICOM standard to incorporate proton arc delivery; (5) working with the TPS and Oncology Information System (OIS) software companies to support the planning and recording of the arc delivery; and (6) developing the new proton arc QA devices for implementing a comprehensive QA program.

Conclusions

This study evaluated the performance of the first prototype of proton arc delivery based on an existing clinical proton therapy system. The measurement and simulation results indicate that the arc delivery system has the potentials to be within clinical requirements. Such findings also demonstrate its clinical feasibility and pave the road for the future implementation of this novel treatment technique in clinical settings.

Financial support

This study is supported by Ion Beam Application S.A. (IBA, Brussels, Belgium) and Beaumont Health Herb and Betty Fisher Research Seed Grant Award.

Conflict of interest

A patent related to SPArc has been filed.

Appendix A. Supplementary data

Supplementary data to this article can be found online at https://doi.org/10.1016/j.radonc.2019.04.032.

References

[1] Lomax A. Intensity modulation methods for proton radiotherapy. Phys Med Biol 1999;44:185–205.
[2] Lomax AJ et al. Intensity modulated proton therapy: a clinical example. Med Phys 2001;28:317–24.
[3] Group, P.T.C.-O., Particle therapy facilities in operation (October 2018).
[4] Zhang XD et al. Intensity-modulated proton therapy reduces the dose to normal tissue compared with intensity-modulated radiation therapy or passive scattering proton therapy and enables individualized radical radiotherapy for extensive stage IIIB non-small-cell lung cancer: a virtual clinical study. Int J Radiat Oncol Biol Phys 2010;77:357–66.
[5] Ding X et al. A comprehensive dosimetric study of pancreatic cancer treatment using three-dimensional conformal radiation therapy (3DCRT), intensity-modulated radiation therapy (IMRT), volumetric-modulated radiation therapy (VMAT), and passive-scattering and modulated-scanning proton therapy (PT). Med Dosim 2014;39:139–45.
[6] Trofimov A et al. Radiotherapy treatment of early-stage prostate cancer with IMRT and protons: a treatment planning comparison. Int J Radiat Oncol Biol Phys 2007;69:444–53.
[7] Cozzi L et al. A treatment planning comparison of 3D conformal therapy, intensity modulated photon therapy and proton therapy for treatment of advanced head and neck tumours. Radiother Oncol 2001;61:287–97.
[8] Ding X et al. Have we reached proton beam therapy dosimetric limitations? - A novel robust, delivery-efficient and continuous spot-scanning proton arc (SPArc) therapy is to improve the dosimetric outcome in treating prostate cancer. Acta Oncol 2018;57:435–7.
[9] Moignier A et al. Theoretical benefits of dynamic collimation in pencil beam scanning proton therapy for brain tumors: dosimetric and radiobiological metrics. Int J Radiat Oncol Biol Phys 2016;95:171–80.
[10] Liu W et al. Influence of robust optimization in intensity-modulated proton therapy with different dose delivery techniques. Med Phys 2012;39:3089.
[11] Liu W et al. Effectiveness of robust optimization in intensity-modulated proton therapy planning for head and neck cancers. Med Phys 2013;40:051711.
[12] Langen K, Zhu M. Concepts of PTV and robustness in passively scattered and pencil beam scanning proton therapy. Semin Radiat Oncol 2018;28:248–55.
[13] Lomax AJ. Intensity modulated proton therapy and its sensitivity to treatment uncertainties 1: the potential effects of calculational uncertainties. Phys Med Biol 2008;53:1027–42.
[14] Unkelbach J et al. Reducing the sensitivity of IMPT treatment plans to setup errors and range uncertainties via probabilistic treatment planning. Med Phys 2009;36:149–63.
[15] Fredriksson A, Forsgren A, Hardemark B. Minimax optimization for handling range and setup uncertainties in proton therapy. Med Phys 2011;38:1672–84.
[16] Liu W et al. Robust optimization of intensity modulated proton therapy. Med Phys 2012;39:1079–91.
[17] Cao W et al. Proton energy optimization and reduction for intensity-modulated proton therapy. Phys Med Biol 2014;59:6341–54.
[18] van de Water S et al. Shortening delivery times of intensity modulated proton therapy by reducing proton energy layers during treatment plan optimization. Int J Radiat Oncol Biol Phys 2015;92:460–8.
[19] Ding X et al. Redefine the role of range shifter in treating bilateral head and neck cancer in the era of Intensity Modulated Proton Therapy. J Appl Clin Med Phys 2018;19:749–55.
[20] Ding X et al. Spot-Scanning Proton Arc (SPArc) therapy: the first robust and delivery-efficient spot-scanning proton arc therapy. Int J Radiat Oncol Biol Phys 2016;96:1107–16.
[21] Li X et al. Improve dosimetric outcome in stage III non-small-cell lung cancer treatment using spot-scanning proton arc (SPArc) therapy. Radiat Oncol 2018;13:35.
[22] Ding X et al. TH-AB-605-05: improve the dosimetric outcome in treating bilateral head and neck cancer treatment using a novel robust and delivery efficient spot scanning proton arc therapy: a feasibility study. Med Phys 2017;44:3277.
[23] Van de Walle J et al. The S2C2: from source to extraction. In: Proc. Int. Conf. on Cyclotrons and Their Applications (Cyclotron2016). p. 21.
[24] Arjomandy B et al. An overview of the comprehensive proton therapy machine quality assurance procedures implemented at The University of Texas M. D. Anderson Cancer Center Proton Therapy Center-Houston. Med Phys 2009;36:2269–82.
[25] Pidikiti R et al. Commissioning of the world's first compact pencil-beam scanning proton therapy system. J Appl Clin Med Phys 2018;19:94–105.

[26] Lin L et al. A novel technique for measuring the low-dose envelope of pencil-beam scanning spot profiles. Phys Med Biol 2013;58:N171–80.
[27] Both S et al. Development and clinical implementation of a universal bolus to maintain spot size during delivery of base of skull pencil beam scanning proton therapy. Int J Radiat Oncol Biol Phys 2014;90:79–84.
[28] Ding X et al. A novel deliver sequence and efficiency optimization algorithm for Spot Scanning Proton Arc therapy. In: Proceedings of the 57 Annual Meeting of the Particle Therapy Cooperative Group (PTCOG). p. 25.
[29] Low DA et al. A technique for the quantitative evaluation of dose distributions. Med Phys 1998;25:656–61.
[30] Li H et al. Use of treatment log files in spot scanning proton therapy as part of patient-specific quality assurance. Med Phys 2013;40:021703.
[31] Tang S et al. Effect of intrafraction prostate motion on proton pencil beam scanning delivery: a quantitative assessment. Int J Radiat Oncol Biol Phys 2013;87:375–82.
[32] Meier G et al. Independent dose calculations for commissioning, quality assurance and dose reconstruction of PBS proton therapy. Phys Med Biol 2015;60:2819–36.